10ème Congrès Français d'Acoustique
Lyon, 12-16 Avril 2010

A deconvolution method based on wavelets to improve detection in ultrasonic tomography

Matthieu Loosvelt, Philippe Lasaygues

Laboratory of Mechanics and Acoustics, UPR CNRS 7051, 13402 Marseille Cedex 20, {loosvelt, lasaygues}@lma.cnrs-mrs.fr}

Wave propagation in soft and hard biological tissues (such as bones) generates ultrasound signals forming packages with different time and frequency signatures. Correlating the complex physical processes involved with these packages means separating the useful information from parasitic one (e.g. electronic noise). This study proposes a way to increase the ultrasound signals resolution, aiming at simultaneously analyzing the time and frequency parameters, by using a wavelet decomposition of the signals. We also discuss ways to generate suitable transmitted signals correlated with the parameters of the test system. This deconvolution method based on wavelets enables to directly determine the transfer function of the scatterer, and gives improved results compared to more classical schemes.

1 Introduction

Medical imaging is the main field in which ultrasonic computed tomography (UCT) is applied [1]. UCT, which involves the linearisation of the inverse problem of acoustic wave propagation, enables one to find specific response to the problem of soft tissue imaging (dedicated to breast cancer detection [2]) and to the problem of bone imaging (dedicated to bone diseases, infections and cancers [3]). The difficulties raised are somewhat different in the sense that in soft tissues, the very weak fluctuations that have to be quantified suffer of their very low values. This poor echogenic index generally induces low detection probability, for instance in the case of large diffuse mass. In addition, invasive lesions that should not be missed may show a millimetric size. In bone imaging, the difficulties are bound with the very high contrast, which strongly alters the propagation of the ultrasonic waves. There, the solutions consist in optimally assess these non-linear effects in an iterative approach that performs local linearization.

For both domains the wave propagation associated with some physical phenomena makes it necessary to change the methods used for the acquisition of the ultrasonic signals. To overcome these problems, the use of low ultrasound frequencies (≤ 3 MHz) provides an effective possible alternative [4]: when the frequency of the transmitted wave decreases, certain zones turn out to be more homogeneous and the attenuation is also reduced. However, if the depth of the field increases, the resolution of the signals and hence that of the reconstructed images is bound to decrease. Even with low frequencies, the complexity of the wave propagation process generates extremely complex acoustic signals consisting of several packets with different signatures, which it is often difficult to analyze (in terms of the wavepaths, volume, guided or surface waves, and attenuation) and to interpret.

To improve the quality of the signals used either to reconstruct a tomographic image or to characterize the physical processes involved, or both, it is interesting to focus on signal processing. More in particular, in order to obtain a better quantification while extracting characterization information from the received signal, we tried several approaches: filtering, spectrum analysis and a method involving the deconvolution of the signals using a characteristic transfer function of the experimental device [5]. The latter operation improves the information in the high and low frequency ranges. That's why we use an alternative method based on a multi-scale decomposition procedure of the signals, enabling to process all the information available in terms of frequency and time.

However, this analysis alone does not suffice to optimize the signal processing: the acoustic signature of the transmitted wave, i.e. the incident wave reaching the scatterer, also has to match some or all of the wavelets' mathematical properties. We then propose solutions to achieve this goal. Then, we show through simulation and experimental results the usefulness of this "wavelet-based deconvolution" method, in comparison with a more conventional signal processing approach.

2 Acoustical statements

The frequencies used here (1 MHz) where performing UCT on strongly contrasted materials (tumors or bones) are therefore lower than those formerly used in practice (for clinical and other purposes, > 3 MHz). This increases the wavelength of the transmitted wave and decreases the quantity of energy lost during the propagation of the wave. It also increases the depth of penetration of the wave into the medium. The scatterer analyzed will be then taken to consist in a quasi-homogeneous medium. But this reduces the accuracy of the separating power and finally the resolution decreases: it is more difficult on the tomogram to identify details such as boundaries. The propagation of the waves will result in signals with specific characteristics, which will depend on the pathways taken and on the mode of data acquisition (reflection, transmission or diffraction) used. In the case of objects showing a strong contrast with

the background, a large proportion of the incident energy is scattered (or simply reflected) and the transmitted proportion is refracted (deviated) after modal conversion at the interface between the water/scatterer, at various angles. The diffraction will not be isotropic. The various wave packets constituting the signals depend decisively on the pathway taken and on the nature of the waves (compressional or shear waves, surface or guided waves). The idea of using a specific signal processing method is to extract as much information as possible about these various packets by analyzing the time and frequency signatures of the signals. It is therefore necessary to decompose these signals so as to identify their constituents.

3 Material and methods

3.1. Test bench

The benches we generally develop consist in a main symmetrical arm carrying two aligned transducer, which can be moved linearly or turned. These transducers and the analyzed object are then immerged into a water tank. Figure 1 shows a synoptic of this experimental setup.

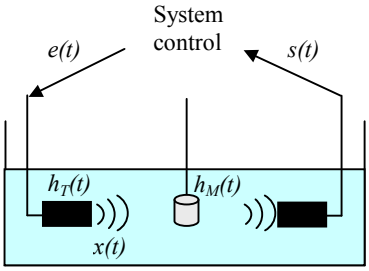

Figure 1: Experimental setup

The electro-acoustic device and the transducers therefore serve as a continuous, linear stationary causal filter. The input and output signals are connected by convolution:

$$s(t) = (x \otimes h_M)(t) = (h_T \otimes e \otimes h_M)(t) \quad (1)$$

where $e(t)$ is the electric signal conveyed to the transmitter, $h_T(t)$ is the pulse response of the two transducers (which is assumed to be known and to be identical), and $h_M(t)$ is the pulse response of the scatterer, which we want to determine.

When the input $x(t)$ cannot be reasonably approximated by a Dirac function, the function $h_M(t)$ has to be deduced from the output measurement $s(t)$ and then, we must deal with deconvolution.

3.2. Wavelet based deconvolution

Wavelet transformation makes it possible to process a signal and to analyze the very local, and much more global, frequency and time parameters. Based on this transformation, a time versus scale diagram can be obtained, giving the evolution of the frequencies with time. Like time-scale processing, wavelet decomposition lends itself very well to detecting and discriminating between signals during the data pre-processing phase as well as the filtering step carried out during an image reconstruction phase.

In most of the cases, $e(t)$ in Figure 1 is comparable to a unit impulse function (i.e. a Dirac delta function), the input will be equal to the transducer's response $x(t) \approx h_T(t)$.

There, let us now generate a wave corresponding to a transmitted signal $x(t)$ having suitable properties for specific processing method, such as wavelet analysis.

If $x(t)$ is a wavelet denoted $\varphi_J(t)$ which is centered on the (dilation) scale denoted J ($J \in Z$) [6], we have:

$$s(t) = \varphi_J(t) \otimes h_M(t) \quad (2)$$

Time-scale decomposition of the signal $s(t)$ on a dyadic grid makes it possible to calculate the coefficients X_j:

$$\begin{aligned} X_j(t) &= s(t) \otimes \phi_{j,0}(t) \\ X_j(t) &= (\varphi_J \otimes h_M)(t) \otimes \phi_{j,0}(t) = h_M \otimes (\varphi_J \otimes \phi_{j,0})(t) \end{aligned} \quad (3)$$

where $\phi_{j,0}(t)$ is a wavelet centered on the scale j ($j \in Z$).

The properties of the wavelet decomposition (an orthogonal decomposition in this case) are such that the coefficients X_j nullify everywhere except for $j = J$:

$$X_j(t) = \begin{cases} (h_M \otimes \delta)(t) = h_M(t) & \text{if } j = J \\ 0 & \text{if } j \neq J \end{cases} \quad (4)$$

If it is possible to process the transfer function of the experimental device in such a way that it is identical to a wavelet function, this method directly yields to the response of the scatterer $h_M(t)$, without any further filtering effects.

3.3. Numerical transmitter signal generation

Experimentally, it is not easy to test the method described in 3.2, because designing the numerical transmitted signal $x(t)$ in wavelets shapes makes it necessary to program an initial function $e(t)$, which has to be filtered by the transducer to obtain a specific wavelet. In our tests, we used a Jaffard wavelet [7] (see Figure 3 for an overview of its temporal and spectral shapes), for its convenient numerical calculation properties. The scale J selected here is −5 due to the frequency sampling of 40 MHz, and the nominal frequency of the transducer of 1 MHz.

During our experiments, we tested several approaches with various levels of success, such as those based on direct deconvolution. Manual determination, which consists in iteratively producing the signal by correcting the quadratic error at each iteration, gave us acceptable results. Meanwhile, using this, we should have to find and generate a new appropriate signal for each new configuration (e.g. transducers changing). We then felt the need for an automated solution, in order to generate as many analyzing wavelets as different test configurations.

In [8], Conil et al. proves that it is possible to reproduce an input waveform for non-linear systems by using a Monte Carlo search guided by a simulated annealing algorithm (itself introduced by Kirkpatrick et al. [9]). The main advantage of this method is that no theoretical model of the system response is required. Meanwhile, in [8], Conil et al. work on a rather simple target waveform (i.e. without too many local extrema).

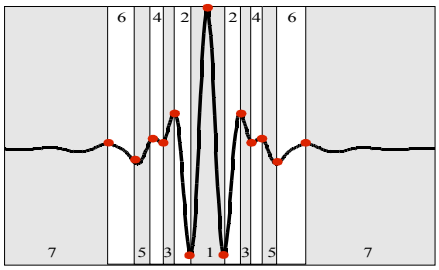

Figure 2: Principle of the "by-zone" simulated annealing and its slicing into "matching zones" (delimited by local extrema)

Then, we have to search how to extend this method to get the desired waveform, provided our targeted wavelet (a Jaffard-Meyer with scale J=-5) contains too many local extrema. We found it was easier to apply a "by-zone" simulated annealing algorithm. Figure 2 shows an illustration of the process we thought of. We first slice the signal into "matching zones", delimited by local extrema. Then, using the same simulated annealing scheme as described in [8], we first try to match the waveform contained in the first zone, (centered zone, marked as "1" in Figure 2). After it reaches a satisfying level of similitude, we extend the matching process to the next two local extrema of the wavelet (that are symmetrical). We kept repeating this process until we reach the last zone (marked as "7" here in Figure 2). Using this "by-zone" method enables us to keep low the number of local extrema to deal with at each state of the algorithm. It also gives us an opportunity to control more finely the perturbing conditions we have to apply, in order to make the algorithm work as efficiently as possible.

4 Results, simulations and experimentations

4.1. Simulation results for wavelet generation using "by-zone" simulated annealing

We first tested our waveform generation algorithm by numerically simulating it. In this purpose, we have considered a target waveform such as a Jaffard wavelet with J=-5, defined by 2048 samples. We have then created a numerical model of the test bench described in Figure 1 (using a measured $h_T(t)$ as a pulse response), and used our "by-zone" simulated annealing on it. Figure 3 gives a sample of resulting waveform and the corresponding spectral shape we obtained (in dotted black line) compared to the theory (in light gray line).

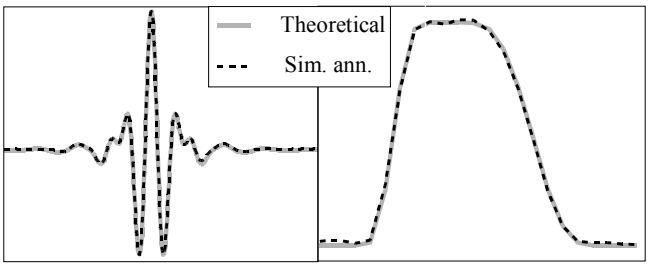

Figure 3: Temporal (left) and spectral (right) shapes obtained using "by-zone" simulated annealing vs. theoretical shapes

Simulations show a good matching between theoretical and experimental obtained shape. Moreover, the algorithm proved to be quite fast on our test configuration (with an average of 13 minutes of executing time). Next step will be to implement this promising algorithm on a practical system.

4.2. Simulation results for wavelet deconvolution

Provided we found possible ways to generate a wavelet-like transfer function for $x(t)$, the method exposed in paragraph 3.2 reveals applicable. Let us take the case of a multi-layer plane interface (water/Plexiglas/water) with thickness D=2 mm and compressional wave velocity c_M=2700 m/s, corresponding to a dioptre constituted of two Dirac localized at $t=t_1$ for the first arrival wave, and $t= t_2$ for the second arrival wave. We have employed both transmitted pulse and Jaffard wavelet at J=-5 as analyzing waveforms.

The case of the interface at a depth of 2 mm is interesting because the wavelength in the water at 1 MHz (equal to 1.5 mm for a compression wave velocity for water of 1500 m/s) is close to the depth, and the signals have therefore merged, as shown in Figure 4. These signals were then decomposed into wavelet functions (several scales j). The maximum coefficients of the dyadic grid were used to identify the scale j, where the echoes are separated, and the time of flight $\Delta t=t_2-t_1$ was calculated (cf. Figure 5).

Table 1 compares the thickness calculated for both analyzing waves. The discrimination based on the transmitted pulse is more difficult (the error is about 73%), whereas using the wavelet-based deconvolution method, it is far more efficient: the error at the interface is only about 8%. Despite these first results gave us a real improvement in terms of resolution, we are still working on the detection method to give even more refined estimation of the thickness (our targeted error percentage is 1 to 2% for thickness below or equal to the system wavelength in water (for recall, here, 1.5 mm)).

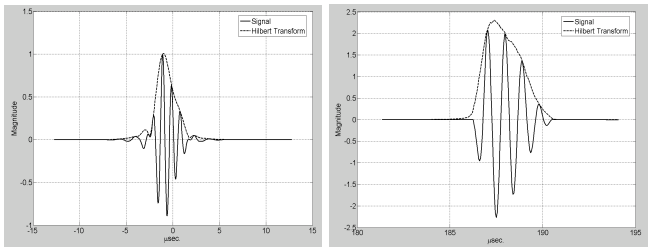

Figure 4: Simulated ultrasonic signals transmitted in plane interfaces; wavelet at J =-5 (left), transmitted pulse (right)

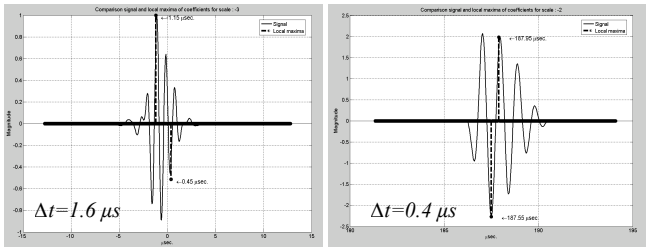

Figure 5: Dyadic grid corresponding to the scale J of non-zero coefficients; wavelet J = -5 (left), transmitted pulse (right)

Real thickness (mm)	Calculated thickness (mm) (error %) $D=(\Delta t * c_M)/2$	
	Wavelet	Transmitted Pulse
2	2.16 (8 %)	0.54 (73 %)

Table 1: Comparison of thickness obtained using the two different analyzing waveforms

4.3. Experimental wavelet deconvolution

We then have experimented the wavelet deconvolution using a sample that was a non-circular homogeneous isotropic tube made of artificial resin (NEUKADUR ProtoCast 113^{TM}). The signals were containing 1024 distributed samples occurring every 50 ns (frequency rate of 20 MHz). The nominal frequency of the transducer was 1 MHz. Figure 6 shows the tomograms given by both analyzing waves.

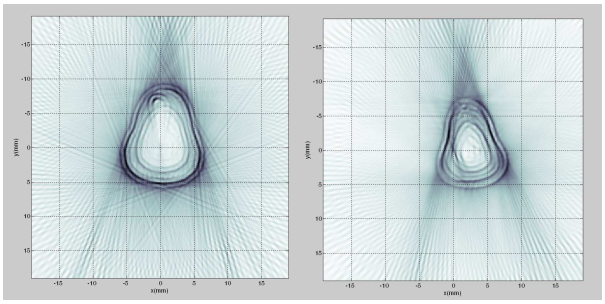

Figure 6: Ultrasonic computed tomography of a non-circular elastic tube. Tomogram with 300 x 300 pixels using a manually generated wavelet at J=-5 (left) or a transmitted pulse (right)

After performing wavelet-based decomposition on the all cross-sectional signals received, the definition of the outer and inner boundaries of the cylinder was obtained with a much better resolution than with the use of the transmitted pulse. This leads us to conclude that using wavelet-based deconvolution is a promising technique in order to obtain better resolution in ultrasonic computed tomography.

References

[1] S. Mensah, J.-P. Lefebvre, ”Enhanced Compressibility Tomography”, IEEE Trans. on Ultras., Ferroelec., Freq. Contr., Vol. 44, No. 66, pp. 1245-1252, 1997.

[2] E. Franceschini, S. Mensah, L. Le Marrec, P. Lasaygues, "An optimization method for quantitative impedance tomography", IEEE Trans. on Ultras., Ferroelec., and Freq. Contr., - Special Issue on High Resolution Ultrasonic Imaging in Industrial, Material and Biomaterial Applications, vol. 54 (8), pp. 1578-1588, 2007.

[3] P. Lasaygues, E. Ouedraogo, J.-P. Lefebvre, M. Gindre, M. Talmant, P. Laugier, "Progress toward in vitro quantitative imaging of human femur using Compound Quantitative Ultrasonic Tomography", Phys. Med. Biol., vol. 50 (11), pp. 2633-2649, 2005.

[4] P. Lasaygues, J.-P. Lefebvre, "Cancellous and cortical bone imaging by reflected tomography", Ultras. Im., vol. 23, pp. 55-68, 2001.

[5] P. Lasaygues, J.-P. Lefebvre, S. Mensah, "High Resolution Low Frequency Ultrasonic Tomography Ultrasonic Imaging", Ultras. Im., vol. 19, pp. 278-293, 1997.

[6] P. Lasaygues, J.-P. Lefebvre, S. Mensah, "Deconvolution and wavelet analysis on ultrasonic reflexion tomography", Topics On Non Destructive Evaluation Series B. Djordjevic and H. Dos Reis, Series Editors, III International Workshop - Advances in Signal Processing for NDE of Materials, in X. Maldague volume 3 Technical Ed, pp. 27-32, ASNT, 1998.

[7] S. Jaffard, "Construction of Wavelets in open sets", Proc. Conf. Wavelets, Time-frequency Method and phase Space, Marseille, 14-18 dec. 1987.

[8] F. Conil, D. Gibert, F. Nicollin, "Non-linear synthesis of input signals in ultrasonic experimental setups", J. Acoust. Soc. Am., pp. 246-252, Jan 2004.

[9] S. Kirkpatrick, C.D. Gellatt, M.P. Vecchi, "Optimisation by simulated annealing", Science 220, pp. 671-680, 1983.